HHS Public Access

Author manuscript

Nat Struct Mol Biol. Author manuscript; available in PMC 2012 May 01.

Published in final edited form as:

Nat Struct Mol Biol. ; 18(11): 1196–1203. doi:10.1038/nsmb.2128.

Structure and nucleosome interaction of the yeast NuA4 and Piccolo-NuA4 histone acetyltransferase complexes

Johnathan R. Chittuluru[1], **Yuriy Chaban**[1], **Julie Monnet-Saksouk**[2], **Michael J. Carrozza**[3], **Vasileia Sapountzi**[2], **William Selleck**[4], **Jiehuan Huang**[4], **Rhea T. Utley**[2], **Myriam Cramet**[2], **Stephane Allard**[2], **Gang Cai**[1], **Jerry L. Workman**[5], **Michael G. Fried**[6], **Song Tan**[4], **Jacques Côté**[2], and **Francisco J. Asturias**[1]

[1]Department of Cell Biology, The Scripps Research Institute, 10550 North Torrey Pines Road, La Jolla, CA 92037, USA

[2]Laval University Cancer Research Center, Hôtel-Dieu de Québec (CHUQ), 9 McMahon Street, Quebec City, Quebec G1R 2J6, Canada

[3]Laboratory of Structural Biology, National Institute of Environmental Health Sciences, 111 T. W. Alexander Dr, Research Triangle Park, NC 27709, USA

[4]Center for Eukaryotic Gene Regulation, Department of Biochemistry and Molecular Biology, Pennsylvania State University, 468A North Frear Laboratory, University Park, PA 16802, USA

[5]Stowers Institute for Medical Research, 1000 East 50th Street, Kansas City, MO 64110, USA

[6]Center for Structural Biology, Department of Molecular and Cellular Biochemistry, University of Kentucky, Lexington, KY 40536, USA

Abstract

We have used electron microscopy (EM) and biochemistry to characterize the structure and nucleosome core particle (NCP) interaction of NuA4, an essential yeast histone acetyltransferase (HAT) complex conserved throughout eukaryotes. The ATM-related Tra1 subunit, shared with the SAGA coactivator, forms a large domain joined to a second portion that accommodates the Piccolo catalytic subcomplex and other NuA4 subunits. EM analysis of an NuA4–NCP complex shows the NCP bound at NuA4's periphery. EM characterization of Piccolo and Piccolo–NCP provided further information about subunit organization and confirmed that histone acetylation requires minimal contact with the NCP. A small conserved region at the N-terminus of Piccolo subunit Epl1 is essential for NCP interaction, whereas subunit Yng2 apparently positions Piccolo

Correspondence should be addressed to F.J.A. (asturias@scripps.edu) or J.C. (jacques.cote@crhdq.ulaval.ca).

Author Contributions: M.J.C. and J.M.-S. expressed and purified NuA4 for EM analysis. J.M-S. expressed and purified the SAGA complex; J.M-S., R.T.U., V.S., M.C., and S.A. expressed and purified NuA4 and recombinant component subunits for biochemical analysis and performed all biochemical analyses of NuA4 and component subunits; W.S. produced recombinant NCP; W.S. and J.H. expressed and purified all Piccolo-NuA4 variants and Piccolo-NuA4 in complex with the NCP; M.G.F. performed all analytical ultracentrifugation experiments; Y.C. collected EM data of NuA4 preserved in ice and calculated the RCT 3D reconstruction of NuA4 from stained particles; J.R.C. collected and analyzed all additional EM data and calculated all remaining structures for Piccolo-NuA4 and NuA4; G.C. performed initial quality inspection of NuA4 3D structures with J.R.C and F.J.A.; J.R.C., F.J.A., S.T., and J.C. discussed and interpreted all results; F.J.A. supervised all EM structural analysis; J.R.C. and F.J.A. wrote the manuscript with input from J.C. and S.T.

for efficient acetylation of H4 or H2A tails. Taken together, these results provide an understanding of NuA4 subunit organization and NCP interactions.

Acetylation is perhaps the best characterized of the histone tail covalent modifications that play a critical role in the regulation of chromatin structure. Large histone acetyltransferase (HAT) complexes target specific histone tail lysines, and the role of different HATs is a matter of intense investigation. NuA4, a large HAT comprising 13 unique polypeptide subunits with a combined molecular weight of 1.0 MDa, is the only HAT whose catalytic subunit, Esa1, is required for cell viability in *Saccharomyces cerevisiae*[1,2]. Three NuA4 subunits (Esa1, Yng2, and Epl1) are responsible for NuA4's HAT activity, and they comprise the Piccolo-NuA4 (Piccolo) catalytic subcomplex[3,4]. NuA4 and Piccolo perform targeted and non-targeted histone H4 and H2A acetylation, respectively. NuA4 is well conserved throughout eukaryotes, and its human homologue, TIP60, plays a critical role in DNA damage response and stem cell regulation (reviewed in[5-8]). Biochemical analysis of NuA4 subunit interactions has resulted in a model for organization of the complex (Fig. 1a, adapted from[9,10]) that presents two modules arranged around the scaffold protein Eaf1. Piccolo also exists as a free complex that is responsible for maintaining basal levels of histone H4 and H2A acetylation, an essential cellular function[4]. The remaining NuA4 subunits have been shown to constitute a recruitment module that targets NuA4 participation in a number of DNA transactions, including DNA repair, transcription initiation, and transcription elongation[10-15].

Recent studies have shown that NuA4 often works in tandem with other complexes[9,11,15-17]. For example, NuA4 and the SAGA coactivator complex (whose catalytic subunit Gcn5 preferentially acetylates histones H3 and H2B)[18] can be co-recruited to promoter regions through their single common subunit, the 433 kDa Tra1 polypeptide[11,19]. Alternatively, through separate mechanisms, both complexes can be recruited to the phosphorylated C-terminal domain of elongating RNA polymerase II[15,20,21]. Consistent with a common understanding that chromatin modification precedes chromatin remodeling, NuA4-dependent histone acetylation allows binding of the RSC and SWI/SNF chromatin remodelers and stimulates RSC activity[16,22,23]. RSC and SWI/SNF activities are also stimulated by the HAT function of SAGA. A similar relationship exists between NuA4 and the ATP-dependent SWR1 complex responsible for the incorporation of the H2A.Z histone variant in chromatin[17].

In contrast with the wealth of knowledge available about NuA4's functions and functional interactions, little is known about its structure. Previous studies have elucidated the atomic structures of NuA4 subunit domains, such as the HAT domain of Esa1[24], the Yeats domain of Yaf9[25], and the Eaf3 chromodomain[26,27]. However, no structural information is available for either the full NuA4 or Piccolo complexes. Despite the paramount biological importance of chromatin remodelers and modifiers, little structural information is available about their interactions with their nucleosomal substrates. Several studies focusing on individual NuA4 component subunits have attempted to address the means by which NuA4 binds to the nucleosome, but the general mechanism for this interaction is still poorly understood. In this

study, we applied single-particle EM and biochemistry to determine the structures of NuA4 and Piccolo and to investigate their mode of interaction with the nucleosome core particle.

Results

Structural study of the NuA4 complex by single-particle EM

We purified NuA4 from yeast extracts as reported[4], through a tandem affinity purification (TAP) tag[28] engineered into the C-terminus of its Epl1 subunit (Fig. 1b). Initial EM characterization was performed on NuA4 particles adsorbed onto a continuous amorphous carbon layer and preserved in stain. An average obtained after alignment of stained particle images shows two large NuA4 domains joined by thin connections (Fig. 1c). By applying the random conical tilt (RCT) method[29] to tilt-pair images of stained particles, we were able to calculate an initial 3D structure of NuA4 (Fig. 1d). This RCT volume was used as an initial reference for iterative refinement of a three-dimensional structure of NuA4 calculated from ~35,000 images of NuA4 particles preserved in amorphous ice[30] (Fig. 1e).

The cryo-EM map of NuA4 shows the structure of the complex, free of specimen preservation artifacts (Fig. 1f). The angular distribution of images in the cryo-EM dataset indicates that an adequate number of NuA4 orientations were recorded and analyzed (Supplementary Fig. 1a), and we estimate the resolution of the NuA4 cryo-EM structure to be ~20 Å by the 0.5 Fourier Shell Correlation criterion[31] (Supplementary Fig. 1b). Class averages obtained by reference-free alignment within groups of cryo-images segregated by orientation show good agreement with projections of the cryo-EM NuA4 volume (Supplementary Fig. 2).

NuA4 and SAGA structures and localization of Tra1

Subunit Tra1 accounts for nearly half (~43%) of the total mass of NuA4. Biochemical studies[10] have detected only limited contacts between Tra1 and other NuA4 subunits (Fig. 1a), which suggested that Tra1 might constitute a sizable portion of one of the large NuA4 domains. Direct localization of Tra1 by deletion mapping is complicated because the subunit is essential in all of its length[32]. However, the location of Tra1 within the yeast SAGA HAT complex has been determined by EM analysis,[33] and we decided to compare the NuA4 and SAGA structures to elucidate the distribution of Tra1 density within NuA4. We purified SAGA by TAP tagging and recorded EM images of SAGA particles preserved in stain. A 2D map of SAGA (Fig. 2a, left) shows that the top portion of the SAGA structure is formed by two well ordered domains that show a striking resemblance in shape and density distribution to the entirety of the NuA4 structure (Fig. 2a, right).

There is no evident sequence homology between NuA4 and SAGA subunits other than Tra1, making a correspondence between the NuA4 and SAGA structures that extends beyond Tra1 an interesting and unexpected finding. Fortunately, besides determining the location of the Tra1 N-terminus by immunolabeling, the previous EM study of SAGA also established the overall boundaries for Tra1-related density by analyzing the structure of a SAGA subunit deletion mutant in which Tra1 was absent[33]. Tra1 occupies the upper left domain of the SAGA projection map (circled in Fig. 2a), which is nearly identical to the left half of the

NuA4 projection map. Therefore, we conclude that most of this half of NuA4, is formed by Tra1. Consequently, the other half of the NuA4 map must contain the majority of the remaining NuA4 subunits, including the catalytic Piccolo subcomplex.

Localization of the Piccolo subcomplex

We employed several approaches to localize the Piccolo subcomplex. First, we purified NuA4 from a mutant yeast strain lacking the C-terminus (residues 486–833) of the Epl1 subunit. This Epl1 truncation separates Piccolo subunits from the remainder of NuA4[4], and this smaller (ΔPiccolo) NuA4 can be purified by Eaf1–TAP[10] (Supplementary Fig. 3). Comparing 2D EM maps of ΔPiccolo and wild-type NuA4 shows that whereas the Tra1 domain retains its structural integrity, the other half of the NuA4 structure appears considerably reduced in the absence of Piccolo (Fig. 2b). Therefore, Tra1 and Piccolo are located in opposite domains of the NuA4 structure and, in agreement with results from biochemical analysis of subunit interactions in NuA4 (Fig. 1a), do not contact each other directly[10].

Localization of the Epl1 Piccolo subunit provided further information about the arrangement of Piccolo within NuA4. A calmodulin binding peptide (CBP) left on the C-terminus of the Piccolo subunit Epl1 after TAP tagging was targeted with an anti-CBP polyclonal antibody (Open Biosystems). A class average calculated from images of antibody-decorated NuA4 particles shows diffuse density near the middle of the lower side of the NuA4 structure (Fig. 2c), indicating that the Epl1 C-terminus is likely mobile and located in that general area. A second labeling experiment was carried out with a gold-conjugated calmodulin probe (Au–CAM)[34,35] also directed toward the CBP tag on Epl1. Roughly 18% of NuA4 particles show a small, well-defined area of high density with a radius of ∼2 nm, matching the expected size of the gold cluster after incubation with Au–CAM and calcium (Fig. 2d). To establish the statistical relevance of the signal attributed to the gold probe, we calculated a difference map by subtracting a normalized 2D average of NuA4 imaged with gold in the absence of calcium (calcium is essential for the calmodulin–CBP binding interaction) from an average obtained from gold-labeled NuA4 particles. The brightest peak in this difference map corresponds in position to the gold density apparent in the average obtained from images of gold-labeled NuA4 and has intensity above 3 standard deviations (Fig. 2d and Supplementary Fig. 4). The results from gold cluster and antibody labeling of the Epl1 C-terminus agree, and the gold cluster labeling more precisely localizes the C-terminus of the Epl1 Piccolo subunit to the non-Tra1 (right) domain of the NuA4 structure, near the inter-domain boundary.

Interaction of NuA4 with the nucleosome core particle

Our next goal was to investigate the interaction between NuA4 and the NCP. NuA4 particles preserved in stain were imaged following incubation with a 9-fold molar excess of recombinant NCPs formed from full-length *Xenopus* recombinant histones and mouse mammary tumor virus long terminal repeat NucB DNA[36,37]. The NuA4 concentration in the EM samples (∼20 nM) was close to the estimated K_d for NuA4–NCP interaction and, accordingly, only ∼5% of NuA4 particles from this experiment were bound to NCPs. However, a class average calculated from images of NuA4–NCP complexes clearly shows

NCP density adjacent to the position previously identified by labeling of Epl1 with anti-CBP antibodies and Au–CAM (Fig. 2e). The NCP density appears partially disordered (the diameter of the NCP density is somewhat smaller than the X-ray structure of the NCP) indicating a flexible interaction with NuA4. The approximate location of this position can be mapped to the cryo-EM 3D structure of NuA4 (Fig. 2f, black arrowhead).

Characterization of the Piccolo–NCP interaction

The results from our NuA4 labeling experiment with the NCP indicated that, at least under the conditions of our EM experiment, NuA4 and the NCP interact with a 1:1 stoichiometry. To determine if this stoichiometry also applied to the Piccolo–NCP complex in solution, we undertook sedimentation equilibrium (analytical) ultracentrifugation (AUC) studies of Piccolo and the Piccolo–NCP complex. For each of the samples analyzed (Piccolo, NCP, and Piccolo–NCP complex), the AUC curves are very well described by a single species. These AUC results establish that Piccolo in solution contains single copies of Esa1, Epl1, and Yng2. Consistent with the EM observations about NuA4 interaction with the NCP, the AUC results show that Piccolo also binds the NCP with a 1:1 stoichiometry (Fig. 3a, Table 1).

Analysis of EM images of Piccolo–NCP particles preserved in stain resulted in a class average in which densities corresponding to the NCP and to Piccolo could be readily identified (Fig. 3b). Features in the Piccolo–NCP projection map appeared blurred, suggesting some conformational variability in the Piccolo–NCP particles. Focusing alignment on the NCP or Piccolo portions of Piccolo–NCP images resulted in better-defined maps for interacting Piccolo and NCP. When Piccolo–NCP image alignment is focused on Piccolo, the projection structure of Piccolo bound to the NCP shows a small particle with well-defined features lying adjacent to blurred NCP density (Fig. 3c). To verify this result, we imaged Piccolo in the absence of the NCP. The resulting Piccolo projection map (Fig. 3d) shows strong resemblance to the Piccolo average obtained from the Piccolo–NCP images. We also imaged an additional Piccolo variant (Piccolo v03) that differed from Piccolo v07 and v55 by inclusion of two additional portions of Epl1 (residues 1–49 and 381–485) and the Yng2 PHD domain (residues 221–282) (see Supplementary Figs. 5 through 7 for additional details about the composition and structural analysis of Piccolo deletion variants). The Piccolo v03 projection structure (Fig. 3e) suggests that additional regions of Epl1 and Yng2 contribute density (highlighted by the yellow arrowhead) that is proximal and possibly connected to the portion of the Piccolo structure involved in direct contact with the NCP.

When Piccolo–NCP image alignment is focused on NCP density, the resulting Piccolo–NCP projection map shows a well-defined nucleosome in contact with blurred Piccolo density. Interestingly, in this map the NCP appears somewhat flat along the side contacted by Piccolo (Supplementary Fig. 8a, flat portion flanked by yellow arrowheads). A 2D map of the NCP alone calculated from images recorded from the same EM samples used to generate the Piccolo–NCP 2D map is remarkably similar to the NCP portion of the Piccolo–NCP 2D map and clearly shows the same flat feature along the top face (Supplementary Fig. 8b). Comparison with a projection of the nucleosome X-ray structure in approximately the same

orientation (Supplementary Fig. 8c) underscores that the flat side of the nucleosome is defined by the entry and exit points of nucleosomal DNA across from the dyad. Because the NCP portion of the Piccolo–NCP 2D map appears circular, except around the area where the NCP is contacted by Piccolo, this 2D analysis establishes the approximate rotational orientation of the NCP in the Piccolo–NCP 2D map, indicating that Piccolo contacts the NCP at a position roughly across (± ∼20°) from the dyad.

The recombinant v07 Piccolo construct used in the EM and AUC studies was shown to be fully active on chromatin substrates[3,4] and comprised full-length, 6 × His-tagged Esa1 (residues 2–445) but truncated forms of Epl1 and Yng2. The Epl1 truncation comprised residues 51–380 (conserved EPcA domain) and lacked 453 C-terminal residues; the Yng2 truncation mutant comprised residues 2–218, which did not include the Yng2 PHD domain (as with Piccolo v55 in Supplementary Fig. 5). Therefore, a stable 1:1 stoichiometric Piccolo–NCP complex is formed even in the absence of both the Epl1 C-terminus and the Yng2 PHD domain.

A 3D map of the Piccolo–NCP complex determined using the RCT method (Fig. 3f) also helped us understand the relative spatial arrangement of Piccolo and the NCP. The NCP X-ray structure[38], or an RCT reconstruction of the NCP determined from images of free nucleosomes present in the Piccolo–NCP EM samples (not shown), could be directly docked into the RCT 3D structure of the Piccolo–NCP complex. As was the case with the 2D analysis, the NCP orientation indicated by the 3D docking suggests that Piccolo interacts with a region of the NCP approximately opposite the dyad (Fig. 3g and Supplementary Fig. 8d). This orientation of the NCP in the Piccolo–NCP complex would place an extended Piccolo density near the histone-fold domain of histone H4 (H4HFD), which has been previously identified as the binding site for the Esa1 Piccolo subunit[39].

To reconcile the information about the Piccolo–NCP interaction with our results about the location of Piccolo within the NuA4 structure and the NuA4–NCP interaction, we sought to dock the Piccolo–NCP RCT map into the larger NuA4 3D structure. Because the resolution of the Piccolo–NCP RCT map is limited as a result of the flexible interaction between Piccolo and the NCP, which in turns limits the accuracy of orientation parameters used to calculate the RCT Piccolo–NCP map, we calculated an RCT reconstruction of Piccolo alone. We docked this structure into the cryo-EM NuA4 map (Supplementary Fig. 9a) and found that Piccolo could be docked in a unique position and orientation within the right half of the NuA4 structure. Docking of the lower resolution Piccolo–NCP map was then guided by the position of Piccolo (Supplementary Fig. 9b). The position of the Piccolo–NCP map determined through this stepwise procedure is consistent with the observed interaction between NuA4 and the NCP (Fig. 2e and Supplementary Fig. 9c). Finally, since our results suggest that Piccolo might have extended contacts with histones and DNA, we pursued a series of biochemical experiments designed to identify elements necessary for binding of NuA4 and Piccolo to the NCP.

Nucleosome binding and chromatin acetylation by NuA4

We pursued several experiments to investigate in more detail how NuA4 and Piccolo bind the NCP and which subunits make the greatest contributions to binding.

First, we determined that the chromodomain subunit Eaf3 does not play a primary role in NuA4 binding to chromatin *in vivo*. When NuA4 is affinity purified from cell extracts in low-salt conditions, a sizeable amount of all four core histones is detected (Fig. 4a). However, when this is repeated in a mutant strain (*eaf1*) that disconnects Eaf3 from Epl1 (Fig. 1a;[10]), histones no longer co-purify with the Eaf3-containing module (Fig. 4a, lane 2).

Second, we investigated Epl1 involvement in NCP binding by performing mobility shift assays with constructs comprising different portions of Epl1 and NCPs. We have previously shown that a recombinant Esa1–Epl1 heterodimer has much stronger acetylation activity on free histones and chromatin when compared to Esa1 alone, whereas inclusion of Yng2 in Piccolo drives acetylation only toward chromatin[4]. Mobility shift assay results now indicate that the Epl1 N-terminal region, encompassing the conserved EPcA domain[4,40], has a very strong affinity for the NCP and that in its presence, Epl1 forms a stable complex with mononucleosomes (Fig. 4b).

Third, we investigated the effect of Piccolo subunit interactions on the HAT activity of Esa1. We started by obtaining evidence for simultaneous association of Esa1 and Yng2 to the Epl1 N-terminal region by mixing the three recombinant proteins together followed by GST pull down analysis. We could detect efficient binding of both Esa1 and Yng2 (Fig. 4c), since the Epl1 N-terminal region independently binds Esa1 and Yng2, physically linking them together in Piccolo NuA4[3,4]. We then analyzed how interaction with Epl1 and Yng2 modulates the HAT activity of Esa1 toward free histones and a chromatin substrate (Fig. 4d, keeping the amount of Esa1 protein constant). As previously shown, recombinant Esa1 (rEsa1) can only acetylate free histones[1]. The addition of Yng2 does not affect Esa1 activity, as expected, since no direct interaction between the two proteins was detected[4]. Addition of Epl1 to Esa1 (rEsa1 + rEpl1) had a striking positive effect on its activity toward free histones but did not enable activity on chromatin. This indicates that Epl1 association with Esa1 increases its specific enzymatic activity, but that the strong affinity of Epl1 for the NCP is non-productive in positioning Esa1 to acetylate H4 or H2A tails. Finally, a mixture of all three proteins (rEsa1 + rEpl1 + rYng2) increased Esa1 specific activity toward free histones to about the same level as Epl1 alone, but acetylation of chromatin was also detected in the presence of Yng2. These data suggest that while Epl1–Esa1 dimers bind efficiently to nucleosomes, Yng2 is required to position Piccolo in a specific orientation that places H4 or H2A histone tails in a productive location near the Esa1 catalytic site.

Fourth, we used NCP mobility shift assays to investigate interaction with individual Piccolo subunits (Fig. 4e). The results establish that while Esa1 shows no interaction and tight binding is again observed for the Epl1 N-terminus, Yng2 does seem to directly bind the nucleosome to some detectable level. Furthermore, this interaction does not seem to involve the Yng2 PHD domain (Fig. 4e, lanes 9–11).

Fifth, we used additional NCP mobility shift assays to determine the critical component for interaction between the NCP and the Piccolo complex. The assays were performed on two Piccolo constructs identical in their Yng2 (Yng2ΔPHD 1–220) and Esa1 (Esa1 1–445) polypeptides, but differing in their Epl1 component (Fig. 5a). NCP binding was detected for a construct including Epl1 residues 51–380 (the minimal Epl1 domain required for cell

viability[4]), while no NCP binding interaction was observed for a construct including only Epl1 residues 72–380 (Fig. 5b). These results show that Epl1 residues 51–71 are essential for the Piccolo–NCP binding interaction. In contrast, the Yng2 PHD domain is dispensable for binding of mononucleosomes by a recombinant Piccolo complex (Fig. 5c). The observation from this mobility shift assay that the Yng2 PHD domain has no striking effect on Piccolo's ability to bind nucleosomes is in agreement with the negligible role played by this domain in NuA4 and Piccolo HAT activity toward chromatin[3,4,41]. These observations, along with results from previous and parallel studies[3,4], provide an overview of Epl1 binding interactions (Fig. 5d).

To summarize, in remarkable agreement with our EM observations, these biochemical results indicate that the N-terminal portion of the Epl1 Piccolo subunit plays a primary role in enabling binding of NuA4 to chromatin, with additional Piccolo subunits being important for modulating the Epl1-based interaction and Esa1 HAT activity.

Discussion

The structure of the NuA4 HAT complex comprises two large globular domains joined by multiple connections (Fig 1). One of these domains is mostly formed by Tra1, the largest NuA4 subunit (433 kDa MW, accounting for ∼43% of the mass and ∼48% of the volume of the 1 MDa complex) (Fig. 2). Presumably, most of the remaining subunits, including the Piccolo catalytic subcomplex, are localized in the second NuA4 domain. This is confirmed by the results from antibody and gold-cluster labeling of the Epl1 Piccolo subunit (Fig. 2), and it is further supported by a diminished size and large-scale changes in the structure of the non-Tra1 domain in images of the ΔPiccolo NuA4 mutant, which comprises all NuA4 subunits except those found in the Piccolo subcomplex. Incubation of NuA4 with NCPs results in NCP density adjacent to the non-Tra1 NuA4 domain, again indicating that Piccolo is located in that portion of NuA4 (Fig. 2). The structure of the non-Tra1 NuA4 domain indicates that Piccolo and two other NuA4 subunit complexes identified by biochemical analyses, Eaf5–Eaf7–Eaf3 and Eaf2–Yaf9–Act1–Arp4 (Fig. 1), are in close physical proximity[10]. It has been reported that deletion of the Eaf1 scaffold protein[10] results in a partial NuA4 complex that lacks only Tra1 and Eaf1[15], suggesting that Eaf1 must form most the interface between the two globular NuA4 domains. Despite biochemical evidence that Eaf1 provides most of the contacts that keep together the Piccolo, Eaf3–Eaf5–Eaf7, and Eaf2–Yaf9–Act1–Arp4 subcomplexes[10,14], it seems plausible from their relatively compact arrangement in the NuA4 structure that additional contacts among these three subcomplexes could account for their observed association in cell extracts in the absence of Eaf1[15], which is not detected in affinity-purified complexes[10,14].

Our results also provide structural insight into the interaction of a HAT complex with the NCP. The absence of any large cavities in the NuA4 structure and the direct observation of NCP binding to NuA4 (Fig. 2) indicate that interaction of NuA4 with the nucleosome occurs at the periphery of NuA4. This is in contrast with what we observed for the RSC chromatin-remodeling complex, which binds the nucleosome in an internal cavity where extensive interactions take place[42]. NuA4 binds the nucleosome in a non-enveloping fashion through limited, localized contacts. The nimble interaction between NuA4 and the NCP might

explain how NuA4 could operate in a condensed chromatin environment (*e.g.* the 30 nm fiber). Relaxation of heterochromatin packing following histone tail acetylation by NuA4 may alleviate steric inhibition and provide a platform for bromodomain interaction, allowing complexes like RSC to bind the nucleosome and carry out physical remodeling of chromatin. Future biochemical studies of RSC activity on condensed and relaxed chromatin templates, and in the absence and presence of histone acetylation, could provide evidence to test this hypothesis.

We used a number of binding assays to further investigate the interaction between NuA4 (or Piccolo) and the NCP. Mobility shift assays showed that, on its own, Esa1 made no or only negligible stable contacts with the NCP, whereas Yng2 and Epl1 made observable binding contacts (Fig. 4b, e). The interaction between Epl1 and the NCP was the strongest, and deletion analysis showed that the conserved N-terminus of Epl1 was mainly responsible for interaction with the NCP. Further deletion analysis showed that Epl1 residues 51–71 are required for the binding interaction between Piccolo and the NCP (Fig. 5b). We also obtained evidence that NuA4 association with chromatin *in vivo* is primarily dependent on the presence of the Piccolo subcomplex (Fig. 4a), further supporting the role of Epl1 as the primary chromatin-binding subunit of NuA4. In our model, the chromatin-specific role of Yng2 in stimulating acetylation would be explained by correctly orienting the binding of Epl1–Esa1 to the nucleosome, leading to productive co-localization of the Esa1 catalytic site and H4 or H2A histone tails.

These binding assay results are consistent with our structural observations. EM analysis of a recombinant Piccolo–NCP complex allowed us to determine its 3D structure, which we partially interpreted by docking of an atomic resolution model of the NCP. Piccolo has been reported to bind the H4HFD through the Esa1 HAT subunit[39]. However, in order to account for the increased catalytic efficiency of Piccolo over Esa1 alone (an increase of ∼2–3 orders of magnitude) the authors of that study propose that the Piccolo subunits Epl1 and Yng2 might also contact the nucleosome. Our EM structure of the Piccolo–NCP complex shows a large Piccolo–NCP interface comprising multiple contacts, primarily on one face of the histone octamer, that includes the H4HFD but also extends to possibly include other histones and DNA. This observation is consistent with the hypothesis that Yng2 and/or Epl1 make additional contacts with the nucleosome. Additionally, we note that the Piccolo–NCP interaction we report occurs in the absence of the Yng2 PHD domain, providing structural evidence supporting the hypothesis that the binding interaction between Piccolo and the NCP does not require this domain.

Further insight into Piccolo subunit organization derived from EM analysis of a number of Piccolo variants is also consistent with the description of Piccolo–NCP contacts we propose. Differences between the structures in projection of different Piccolo deletion variants (Supplementary Figs. 5 through 7) suggest that at least some portions of Esa1 are localized in the central region of the Piccolo structure, distal to the area of NCP interaction. On the other hand, portions of Epl1 (and perhaps also the Yng2 PHD domain) are in close proximity to the nucleosome-binding region of Piccolo. These structural observations are based on comparison of 2D structures calculated from images of particles preserved in stain (a low resolution technique), and comparison between the projection structures of different

Piccolo variants highlights regions where density disappears upon subunit deletion, providing only indirect evidence for localization of specific subunits. Nonetheless, taken together with our other structural and biochemical observations, these results are consistent with a model for Piccolo–NCP interaction where Epl1 plays a primary role in binding the NCP, Yng2 stabilizes this interaction and positions the NCP for optimal catalysis, and Esa1 plays a lesser (though catalytically relevant) role in binding and is primarily involved in catalysis.

Finally, one of the most intriguing observations from this study is an uncanny resemblance between the structures of NuA4 and SAGA that extends well beyond what could be explained by the presence of the common Tra1 subunit. The SAGA subunits (Taf5, Taf6, Taf9, Taf10, and Taf12) that presumably comprise part of the SAGA domain that corresponds structurally to the non-Tra1 portion of NuA4[33] share no sequence homology with NuA4 subunits. A search for subunit interaction partners shared by NuA4 and SAGA components failed to identify any. Still, NuA4 and SAGA acetylate nucleosomes and often act in concert in the same environment inside the nucleus[19]. Furthermore, it has been recently shown that NuA4 and SAGA are both recruited to the phosphorylated C-terminal domain of elongating RNA polymerase II[15]. Structural similarities between the two complexes that extend beyond Tra1 may represent convergent evolution of structure highlighting common aspects of two different solutions to a shared set of general molecular functions. Alternatively, it is possible that NuA4 and SAGA may, at some point during their shared roles in DNA transactions, bind to a common interface (perhaps a particular chromatin architecture or another large protein complex) that dictates their structural similarity.

Methods

Purification and electron microscopy of NuA4 and SAGA

NuA4 and SAGA were purified by the TAP method[28] essentially as described[43]. TAP tags were inserted at the C-termini of the Epl1 and Spt7 subunits of NuA4 and SAGA, respectively (for NuA4 purified from an Epl1(1–485) truncation background (ΔPiccolo), the Eaf1 subunit was TAP tagged). Purified complexes were analyzed by SDS–PAGE, and western blot (data not shown, see examples in[17]). In some cases, samples were further purified by gel filtration on a Superose 6 column (GE Healthcare).

EM samples of NuA4 and SAGA preserved in stain were prepared as described[42]. Samples were imaged under low-dose conditions on a field emission gun (FEG) Tecnai F-20 microscope (FEI) (acceleration voltage 120 kV). Images were recorded on a Gatan 4096 × 4096 CCD camera at 50,000 × magnification and ~500 nm underfocus. Two-fold pixel binning resulted in a final pixel size of 4.34 Å. Images of individual NuA4 and SAGA particles (~5,000 for each complex) were selected by hand. Image processing was done using the Spider and SPARX software packages[44,45]. Single-particle images were aligned without a reference and subjected to hierarchical ascendant clustering[46] to produce class averages.

Calculation of 3D NuA4 structures

An initial NuA4 3D map was calculated by the random conical tilt (RCT) method[29] as described[42]. Cryo-EM samples were also prepared as described[42] and imaged under low-dose conditions using a FEG CM200 (Philips/FEI) microscope (acceleration voltage 120 kV). Images were recorded on Kodak SO-163 film at a magnification of 66,000 × and with 0.9–4.0 μm underfocus values. Micrographs were digitized on a Zeiss/SCAIA flat bed densitometer (ZI/Zeiss) using a step size of 7 μm. Digitized images were 4-fold pixel averaged to 4.11 Å per pixel. NuA4 particle images (~35,000) were selected by hand, divided into groups according to defocus, and a cryo-EM map of NuA4 was calculated by projection matching refinement as described[42] using the NuA4 RCT reconstruction as initial reference. Three-dimensional structure interpretation and image rendering were done using UCSF Chimera[47].

Epl1 labeling and NuA4 incubation with the NCP

NuA4 at 20 μg ml^{-1} was incubated for 30 min at 25 °C with a five-fold molar excess of polyclonal anti-CBP antibody (Open Biosystems) targeting the calmodulin binding peptide (CBP) tag on the Epl1 subunit. EM samples were then prepared and imaged as described above. Individual particle images (~23,000) were selected by hand, and ~500 were categorized by visual inspection as images showing the NuA4–anti-TAP interaction. Gold-cluster labeling of Epl1 was done by incubating NuA4 at 20 μg ml^{-1} with a 20-fold molar excess of thiol-protected calmodulin-bioconjugated gold nanoparticles[34,35] for 2 h at 4 °C. Incubation with the gold probe was carried out in the presence and in the absence of calcium, and about 4,000 images from each condition were recorded and analyzed. To form the NuA4–NCP complex, NuA4 at 50 μg ml^{-1} was incubated with a 9-fold molar excess of NCPs reconstituted from full-length recombinant histones from *Xenopus* and mouse mammary tumor virus long terminal repeat NucB DNA[36,37]. EM samples were prepared and imaged as before.

EM characterization of the Piccolo and Piccolo–NCP complexes

Recombinant Piccolo NuA4 complex was expressed in bacteria using a polycistronic vector and purified as described[3,4]. The Piccolo–NCP complex was assembled as described[3]. To promote complex stability, Piccolo–NCP (~215 μg ml^{-1}) was crosslinked for 10 min with 1% (v/v) formaldehyde and quenched with 320 mM glycine. The sample was diluted to a final Piccolo–NCP concentration of 20 μg ml^{-1} before preparing and imaging EM samples as described for stained NuA4 specimens. Images were recorded on film and digitized using a Coolscan 9000 scanner (Nikkon). Individual particle images were selected by hand or by automated particle selection with the TiltPicker and DoGPicker software tools[48].

Analytical ultracentrifugation experiments

Samples equilibrated in 20 mM Tris–Cl pH 8.0, 50 mM KCl, 5 mM 2-mercaptoethanol buffer were brought to sedimentation equilibrium in a Beckman XL-A analytical ultracentrifuge fitted with an AN-60Ti rotor, operating at 4.0 ± 0.1 °C. Five data sets were collected at 260 nm and five at 280 nm for each sample, at three rotor speeds (2,600, 5,900 and 14,200 × g) and three nominal concentrations (0.37, 0.19 and 0.09 mg ml^{-1} for Piccolo;

0.15, 0.07 and 0.04 μg ml^{-1} for the DNA-containing complexes). Absorbance versus radial position data were fit by one- and two-species models using partial specific volumes calculated from the amino acid and nucleic acid compositions of the complexes[49]. Global analysis of multiple data sets was performed with the program PRISM (Graphpad, Inc.).

Piccolo NCP binding and acetyltransferase activity

Bacterial expression vectors for different His–Esa1, GST–Epl1 (1–485), GST–Epl1 (486–832), His–Yng2 (1–282) and His–Yng2 (1–218) have been used before[4], and cloning details are available upon request. Piccolo NuA4 complexes used in the experiments shown in Figs. 3 and 5 were produced by coexpression in *E. coli* and purified as described previously[3]. Single GST- and His-recombinant proteins were expressed and purified on glutathione Sepharose or nickel–agarose beads following standard procedures. His-tagged recombinant proteins were precleared on GST–Sepharose for 1 h at 4 °C prior to pulldown. 300 ng of rEsa1 and 200 ng of rYng2 were incubated (3 h at 4 °C) with 300 ng of appropriate GST fusion (or 1 ng of GST control). Equivalent amounts of input, bound, and free fractions were analyzed by western blot using an anti-HIS antibody (BabCo). For HAT assays, individual soluble recombinant proteins were incubated together at a similar ratio for 15 min on ice and 20 min at 30 °C before the assay, which was done with short oligonucleosomes purified from HeLa cells as previously described[1]. Different mixtures of recombinant proteins were prepared with a constant amount of rEsa1. All values were standardized to the activity of rEsa1 alone on free histones. Data shown in Fig. 4d are representative of two different experiments done in duplicate. For nucleosome binding experiments, a labeled 5S RNA gene was reconstituted in mononucleosomes as described[50]. rEsa1, rEpl1, rYng2 or rPiccolo trimeric complex were incubated with 12.5 ng of total nucleosomes for 30 min at 30 °C. Binding reactions were resolved on a 4% (w/v) PAGE gel in 0.5 × TBE. For measurement of histone copurification with NuA4 from whole cell extracts, wild-type and *EAF1*-deleted Eaf5–TAP strains[10] were fractionated over IgG Sepharose followed by TEV elution, keeping salt concentration at 150 mM. Co-purifying Piccolo subunits and histones were detected by western blot and silver staining after separation by gel electrophoresis.

Supplementary Material

Refer to Web version on PubMed Central for supplementary material.

Acknowledgments

This work was supported by US National Institutes of Health grant R01 GM67167 (F.J.A.), R01 GM060489 (S.T.), RO1 GM070662 (M.G.F.) and fellowship F31 GM086978-01 (J.R.C.), a Canadian Institutes of Health Research (CIHR) grant MOP-14308 (J.C.) and fellowship (V.S.), and a Canada Research Chair (J.C.). We also acknowledge the National Resource for Automated Macromolecular Microscopy.

References

1. Allard S, et al. NuA4, an essential transcription adaptor/histone H4 acetyltransferase complex containing Esa1p and the ATM-related cofactor Tra1p. EMBO J. 1999; 18:5108–5119. [PubMed: 10487762]
2. Clarke AS, Lowell JE, Jacobson SJ, Pillus L. Esa1p is an essential histone acetyltransferase required for cell cycle progression. Mol Cell Biol. 1999; 19:2515–2526. [PubMed: 10082517]

3. Selleck W, Fortin I, Sermwittayawong D, Cote J, Tan S. The Saccharomyces cerevisiae Piccolo NuA4 histone acetyltransferase complex requires the Enhancer of Polycomb A domain and chromodomain to acetylate nucleosomes. Mol Cell Biol. 2005; 25:5535–5542. [PubMed: 15964809]

4. Boudreault AA, et al. Yeast enhancer of polycomb defines global Esa1-dependent acetylation of chromatin. Genes Dev. 2003; 17:1415–1428. [PubMed: 12782659]

5. Avvakumov N, Cote J. The MYST family of histone acetyltransferases and their intimate links to cancer. Oncogene. 2007; 26:5395–5407. [PubMed: 17694081]

6. Fazzio TG, Huff JT, Panning B. An RNAi screen of chromatin proteins identifies Tip60-p400 as a regulator of embryonic stem cell identity. Cell. 2008; 134:162–174. [PubMed: 18614019]

7. Kim J, et al. A Myc network accounts for similarities between embryonic stem and cancer cell transcription programs. Cell. 2010; 143:313–324. [PubMed: 20946988]

8. Sapountzi V, Cote J. MYST-family histone acetyltransferases: beyond chromatin. Cell Mol Life Sci. 2011; 68:1147–1156. [PubMed: 21132344]

9. Doyon Y, Cote J. The highly conserved and multifunctional NuA4 HAT complex. Curr Opin Genet Dev. 2004; 14:147–154. [PubMed: 15196461]

10. Auger A, et al. Eaf1 is the platform for NuA4 molecular assembly that evolutionarily links chromatin acetylation to ATP-dependent exchange of histone H2A variants. Mol Cell Biol. 2008; 28:2257–2270. [PubMed: 18212047]

11. Brown CE, et al. Recruitment of HAT complexes by direct activator interactions with the ATM-related Tra1 subunit. Science. 2001; 292:2333–2337. [PubMed: 11423663]

12. Downs JA, et al. Binding of chromatin-modifying activities to phosphorylated histone H2A at DNA damage sites. Mol Cell. 2004; 16:979–990. [PubMed: 15610740]

13. Altaf M, Auger A, Covic M, Cote J. Connection between histone H2A variants and chromatin remodeling complexes. Biochem Cell Biol. 2009; 87:35–50. [PubMed: 19234522]

14. Mitchell L, et al. Functional dissection of the NuA4 histone acetyltransferase reveals its role as a genetic hub and that Eaf1 is essential for complex integrity. Mol Cell Biol. 2008; 28:2244–2256. [PubMed: 18212056]

15. Ginsburg DS, Govind CK, Hinnebusch AG. NuA4 lysine acetyltransferase Esa1 is targeted to coding regions and stimulates transcription elongation with Gcn5. Mol Cell Biol. 2009; 29:6473–6487. [PubMed: 19822662]

16. Carey M, Li B, Workman JL. RSC exploits histone acetylation to abrogate the nucleosomal block to RNA polymerase II elongation. Mol Cell. 2006; 24:481–487. [PubMed: 17081996]

17. Altaf M, et al. NuA4-dependent acetylation of nucleosomal histones H4 and H2A directly stimulates incorporation of H2A.Z by the SWR1 complex. J Biol Chem. 2010; 285:15966–15977. [PubMed: 20332092]

18. Grant PA, et al. Yeast Gcn5 functions in two multisubunit complexes to acetylate nucleosomal histones: characterization of an Ada complex and the SAGA (Spt/Ada) complex. Genes Dev. 1997; 11:1640–1650. [PubMed: 9224714]

19. Robert F, et al. Global position and recruitment of HATs and HDACs in the yeast genome. Mol Cell. 2004; 16:199–209. [PubMed: 15494307]

20. Pascual-Garcia P, et al. Sus1 is recruited to coding regions and functions during transcription elongation in association with SAGA and TREX2. Genes Dev. 2008; 22:2811–2822. [PubMed: 18923079]

21. Govind CK, Zhang F, Qiu H, Hofmeyer K, Hinnebusch AG. Gcn5 promotes acetylation, eviction, and methylation of nucleosomes in transcribed coding regions. Mol Cell. 2007; 25:31–42. [PubMed: 17218269]

22. Hassan AH, Neely KE, Workman JL. Histone acetyltransferase complexes stabilize swi/snf binding to promoter nucleosomes. Cell. 2001; 104:817–827. [PubMed: 11290320]

23. Hassan AH, et al. Function and selectivity of bromodomains in anchoring chromatin-modifying complexes to promoter nucleosomes. Cell. 2002; 111:369–379. [PubMed: 12419247]

24. Yan Y, Barlev NA, Haley RH, Berger SL, Marmorstein R. Crystal structure of yeast Esa1 suggests a unified mechanism for catalysis and substrate binding by histone acetyltransferases. Mol Cell. 2000; 6:1195–1205. [PubMed: 11106757]

25. Wang AY, et al. Asf1-like structure of the conserved Yaf9 YEATS domain and role in H2A.Z deposition and acetylation. Proc Natl Acad Sci U S A. 2009; 106:21573–21578. [PubMed: 19966225]
26. Sun B, et al. Molecular basis of the interaction of Saccharomyces cerevisiae Eaf3 chromo domain with methylated H3K36. J Biol Chem. 2008; 283:36504–36512. [PubMed: 18984594]
27. Xu C, Cui G, Botuyan MV, Mer G. Structural basis for the recognition of methylated histone H3K36 by the Eaf3 subunit of histone deacetylase complex Rpd3S. Structure. 2008; 16:1740–1750. [PubMed: 18818090]
28. Puig O, et al. The tandem affinity purification (TAP) method: a general procedure of protein complex purification. Methods. 2001; 24:218–229. [PubMed: 11403571]
29. Radermacher M, Wagenknecht T, Verschoor A, Frank J. Three-dimensional reconstruction from a single-exposure, random conical tilt series applied to the 50S ribosomal subunit of Escherichia coli. J Microsc. 1987; 146:113–136. [PubMed: 3302267]
30. Dubochet J, et al. Cryo-electron microscopy of vitrified specimens. Q Rev Biophys. 1988; 21:129–228. [PubMed: 3043536]
31. Saxton WO, Baumeister W. The correlation averaging of a regularly arranged bacterial cell envelope protein. J Microsc. 1982; 127:127–138. [PubMed: 7120365]
32. Knutson BA, Hahn S. Domains of Tra1 important for activator recruitment and transcription coactivator functions of SAGA and NuA4 complexes. Mol Cell Biol. 2011; 31:818–831. [PubMed: 21149579]
33. Wu PY, Ruhlmann C, Winston F, Schultz P. Molecular architecture of the S. cerevisiae SAGA complex. Mol Cell. 2004; 15:199–208. [PubMed: 15260971]
34. Ackerson CJ, Jadzinsky PD, Sexton JZ, Bushnell DA, Kornberg RD. Synthesis and bioconjugation of 2 and 3 nm-diameter gold nanoparticles. Bioconjug Chem. 21:214–218. [PubMed: 20099843]
35. Ackerson CJ, Jadzinsky PD, Jensen GJ, Kornberg RD. Rigid, specific, and discrete gold nanoparticle/antibody conjugates. J Am Chem Soc. 2006; 128:2635–2640. [PubMed: 16492049]
36. Flaus A, Richmond TJ. Positioning and stability of nucleosomes on MMTV 3′LTR sequences. J Mol Biol. 1998; 275:427–441. [PubMed: 9466921]
37. Luger K, Rechsteiner TJ, Richmond TJ. Expression and purification of recombinant histones and nucleosome reconstitution. Methods Mol Biol. 1999; 119:1–16. [PubMed: 10804500]
38. Davey CA, Sargent DF, Luger K, Maeder AW, Richmond TJ. Solvent mediated interactions in the structure of the nucleosome core particle at 1.9 a resolution. J Mol Biol. 2002; 319:1097–1113. [PubMed: 12079350]
39. Berndsen CE, et al. Nucleosome recognition by the Piccolo NuA4 histone acetyltransferase complex. Biochemistry. 2007; 46:2091–2099. [PubMed: 17274630]
40. Stankunas K, et al. The enhancer of polycomb gene of Drosophila encodes a chromatin protein conserved in yeast and mammals. Development. 1998; 125:4055–4066. [PubMed: 9735366]
41. Nourani A, et al. Role of an ING1 growth regulator in transcriptional activation and targeted histone acetylation by the NuA4 complex. Mol Cell Biol. 2001; 21:7629–7640. [PubMed: 11604499]
42. Chaban Y, et al. Structure of a RSC-nucleosome complex and insights into chromatin remodeling. Nat Struct Mol Biol. 2008; 15:1272–1277. [PubMed: 19029894]
43. Carrozza MJ, et al. Histone H3 methylation by Set2 directs deacetylation of coding regions by Rpd3S to suppress spurious intragenic transcription. Cell. 2005; 123:581–592. [PubMed: 16286007]
44. Frank J, et al. SPIDER and WEB: processing and visualization of images in 3D electron microscopy and related fields. J Struct Biol. 1996; 116:190–199. [PubMed: 8742743]
45. Hohn M, et al. SPARX, a new environment for Cryo-EM image processing. J Struct Biol. 2007; 157:47–55. [PubMed: 16931051]
46. Frank J. Classification of macromolecular assemblies studied as ‘single particles’. Q Rev Biophys. 1990; 23:281–329. [PubMed: 2204955]
47. Pettersen EF, et al. UCSF Chimera--a visualization system for exploratory research and analysis. J Comput Chem. 2004; 25:1605–1612. [PubMed: 15264254]

48. Voss NR, Yoshioka CK, Radermacher M, Potter CS, Carragher B. DoG Picker and TiltPicker: software tools to facilitate particle selection in single particle electron microscopy. J Struct Biol. 2009; 166:205–213. [PubMed: 19374019]

49. Daugherty MA, Fried MG. Analysis of transcription factor interactions at sedimentation equilibrium. Methods Enzymol. 2003; 370:349–369. [PubMed: 14712659]

50. Cote J, Utley RT, Workman JL. Basic analysis of transcription factor binding to nucleosomes. Methods In Molecular Genetics. 1995; 6:108–128.

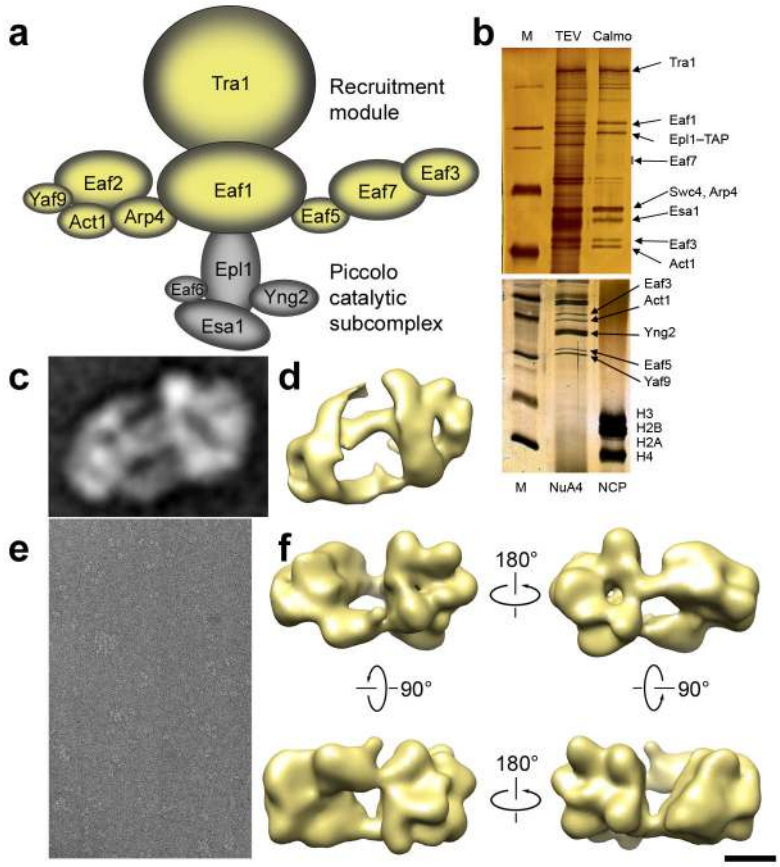

Figure 1. NuA4 subunit organization and EM characterization

(**a**) Model for the organization of NuA4 subunits into functional modules arranged around the Eaf1 scaffold protein (based on[9]). Subunits involved in recruitment of NuA4 to specific loci are colored yellow, and subunits comprising the Piccolo catalytic subcomplex are colored gray. (**b**) SDS–PAGE analysis of NuA4 after TAP purification. The lower gel shows that no histones copurify with NuA4. Subunit Eaf6 (~16 kDa) is not visible since it stains very poorly with silver. (**c**) A 2D class average of NuA4 obtained by reference-free alignment of EM images of particles preserved in stain. (**d**) A view (corresponding to the projection shown in panel **b**) of a 3D reconstruction of NuA4 obtained using the RCT method. The 2D and 3D maps both show a structure comprising two large domains joined by thin connections. (**e**) Representative electron micrograph of NuA4 particles preserved in amorphous ice. (**f**) Different views of a cryo-EM map of NuA4 calculated from ~35,000 individual-particle cryo images. The view in the top left corresponds to the orientation preferentially adopted by particles preserved in stain. Scale bars represent 5 nm (**c**, **d**, and **f**) and 100 nm (**e**).

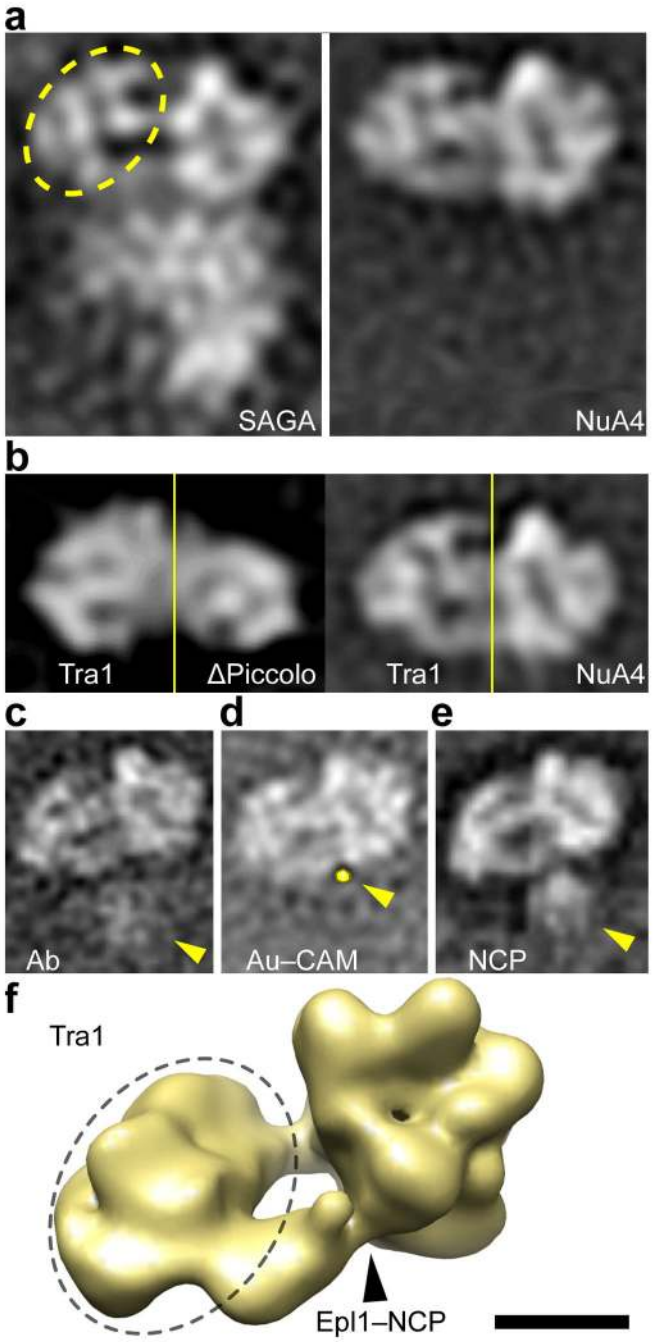

Figure 2. NuA4 subunit organization, interaction with the nucleosome, and structural homology with SAGA

(**a**) 2D class averages obtained by reference-free alignment of SAGA (left) and NuA4 (right) stained particle images. The upper portion of the SAGA structure, whose Tra1 portion is highlighted by a dashed ellipse, is remarkably similar to the NuA4 map. The orientation of NuA4 shown here to match the SAGA map corresponds to a ~20° rotation in the plane of the page from the NuA4 averages presented elsewhere. (**b**) Projection structure of a ΔPiccolo NuA4 mutant (left) next to a projection of wild-type NuA4 (right). The Tra1

portions of the ΔPiccolo and wild-type NuA4 (to the left of the yellow line) are very similar. In contrast, the non-Tra1 portion (to the right of the yellow line) of the ΔPiccolo map is much smaller, reflecting the loss of Piccolo density. (**c**) Immunolabeling of the Epl1 subunit with anti-CBP Ab results in disordered antibody density highlighted by the arrowhead. (**d**) Labeling of the same CBP tag on Epl1 using a calmodulin-derivatized gold cluster results in gold cluster density (yellow arrowhead and false-color overlay highlighting pixels with intensities above 3σ). (**e**) Incubation of NuA4 with nucleosomes results in localized density (highlighted by arrowhead) at the periphery of NuA4 in a position adjacent to the Epl1 subunit. (**f**) The portion of the NuA4 structure corresponding to Tra1 (dashed ellipse) and the location of Epl1 and the NCP binding site (black arrowhead) are highlighted in the 3D cryo-EM map. Scale bars represent 10 nm (**a**, **b**), 13.5 nm (**c**–**e**), and 5 nm (**f**).

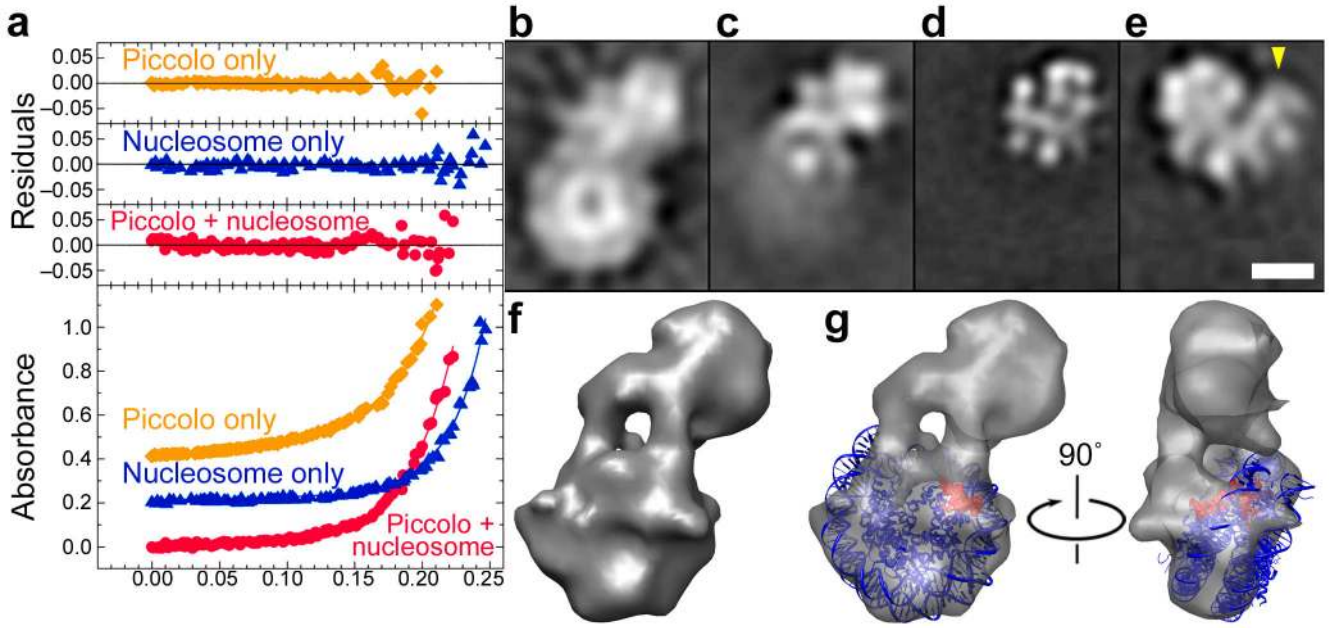

Figure 3. Characterization of the Piccolo–NCP complex by AUC and EM

(**a**). AUC data for Piccolo, NCP, and Piccolo–NCP are shown as orange diamonds, blue triangles, and red circles, respectively, while fitted curves are shown as solid lines. The residuals above document the small difference between the experimental data and the fitted curve used to determine the molecular weights (see Table 1). (**b**) Class average obtained after reference-free alignment of images of individual Piccolo–NCP particles. (**c**) Piccolo class average obtained after masking out NCP density in Piccolo–NCP images (**d**) Piccolo projection map obtained from images of Piccolo alone. (**e**) Piccolo projection map obtained from images of a different Piccolo deletion variant including additional Epl1 and Yng2 domains. (**f**) 3D map of the Piccolo–NCP complex obtained by the RCT method. (**g**) Docking of the X-ray structure of the nucleosome into the Piccolo–NCP 3D map. The H4HFD is highlighted in red. Scale bars represent 5 nm (**b**) through (**e**) and 3.5 nm (**f**, **g**).

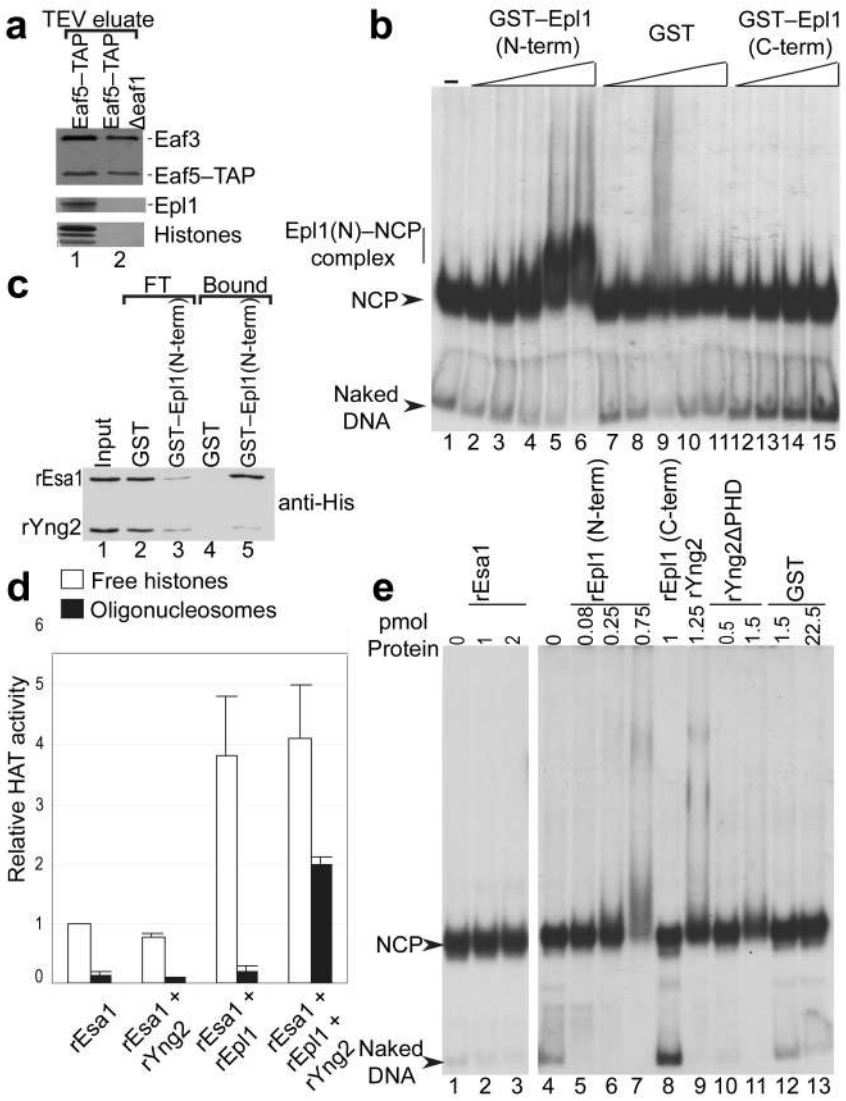

Figure 4. Epl1 N-terminus drives binding to nucleosomes within NuA4, but Yng2 is required for acetylation

(**a**) Physical association of histones with NuA4 requires the Piccolo subcomplex *in vivo*. (**b**) Epl1 N-terminus has strong binding affinity for mononucleosomes. A stable complex is detected between the Epl1 N-terminus and the NCP (lanes 5 and 6). (**c**) GST pull downs using near stoichiometric ratios of the indicated recombinant proteins were carried out and assayed by western blotting. As shown using anti-His antibody for western blots, both rEsa1 and rYng2 are pulled down using GST–Epl1 (N-term). Note that while rEsa1 and rYng2 are pulled down simultaneously using GST–Epl1 (N-term), rEsa1 is more efficiently brought with Epl1. (**d**) Relative HAT activity of rEsa1 alone or in combination with other recombinant proteins present in Piccolo. HAT assays were done on free (open bars) or nucleosomal (black bars) histones. Error bars indicate s.d. (**e**) NCP mobility shift assay showing that the N-termini of rEpl1 and rYng2 are able to interact with nucleosomes while rEsa1 and rEpl1 (C-term) cannot (compare lanes 7 and 9 with 2, 3, and 8).

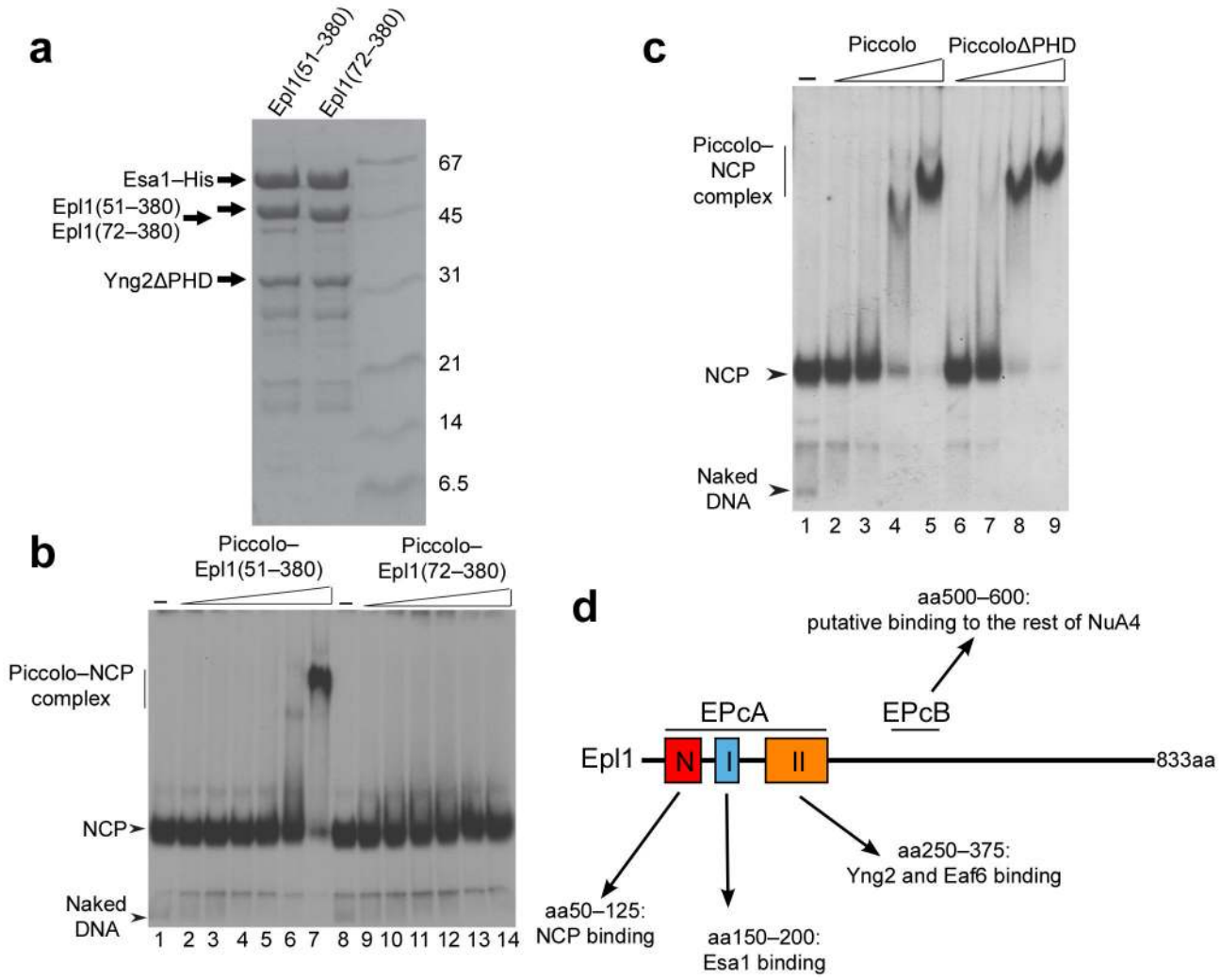

Figure 5. Epl1 residues 51–72 are essential for Piccolo–NCP interaction

(**a**) SDS–PAGE analysis of purified Piccolo constructs comprising full-length Esa1, Yng2ΔPHD, and either Epl1(51–380) or Epl1(72–380). (**b**) Mobility shift assay indicating that Epl1 residues 51–71 are required for the binding interaction between Piccolo and mononucleosomes. (**c**) Mobility shift assay indicating that the Yng2 PHD domain is dispensable for binding of mononucleosomes by the recombinant Piccolo complex. (**d**) Diagram illustrating the residues required for known Epl1 binding interactions elucidated by this and previous or parallel studies[3,4]. The conserved domain EPcA (residues 50–380) can be subdivided in three conserved amino acids clusters with subdomains I and II being responsible for Piccolo assembly by bridging Esa1 together with Yng2 and the subdomain N being the critical NCP binding surface. Amino acid, aa.

Table 1
Molecular weight determination by sedimentation equilibrium

Sample	Expected molecular weight (kDa)	Measured molecular weight (kDa)
Piccolo	117.7	115 ± 6.0
NCP	204.9	209.3 ± 8.3
Piccolo–NCP	322.6	317.4 ± 19.2

Expected vs. experimental molecular weights of 1:1:1 Piccolo, NCP, or Piccolo–NCP complex determined by AUC. Expected molecular weights are calculated for a 1:1:1 Epl1–Yng2–Esa1 Piccolo complex and for a 1:1 Piccolo–NCP complex.